Supplementary Information

Staged decline of neuronal function *in vivo* in an animal model of Alzheimer's Disease

Christine Grienberger[1]*, Nathalie L. Rochefort[1]*, Helmuth Adelsberger[1], Horst A. Henning[1], Dan N. Hill[1], Julia Reichwald[2], Matthias Staufenbiel[2] and Arthur Konnerth[1]

*These authors contributed equally to this work

[1]Institute of Neuroscience and Center for Integrated Protein Science, Technical University Munich, Biedersteinerstr. 29, 80802 Munich, Germany

[2]Novartis Institutes for Biomedical Research, 4002 Basel, Switzerland.

- **Supplementary Figures S1-10**
- **Supplementary Methods**

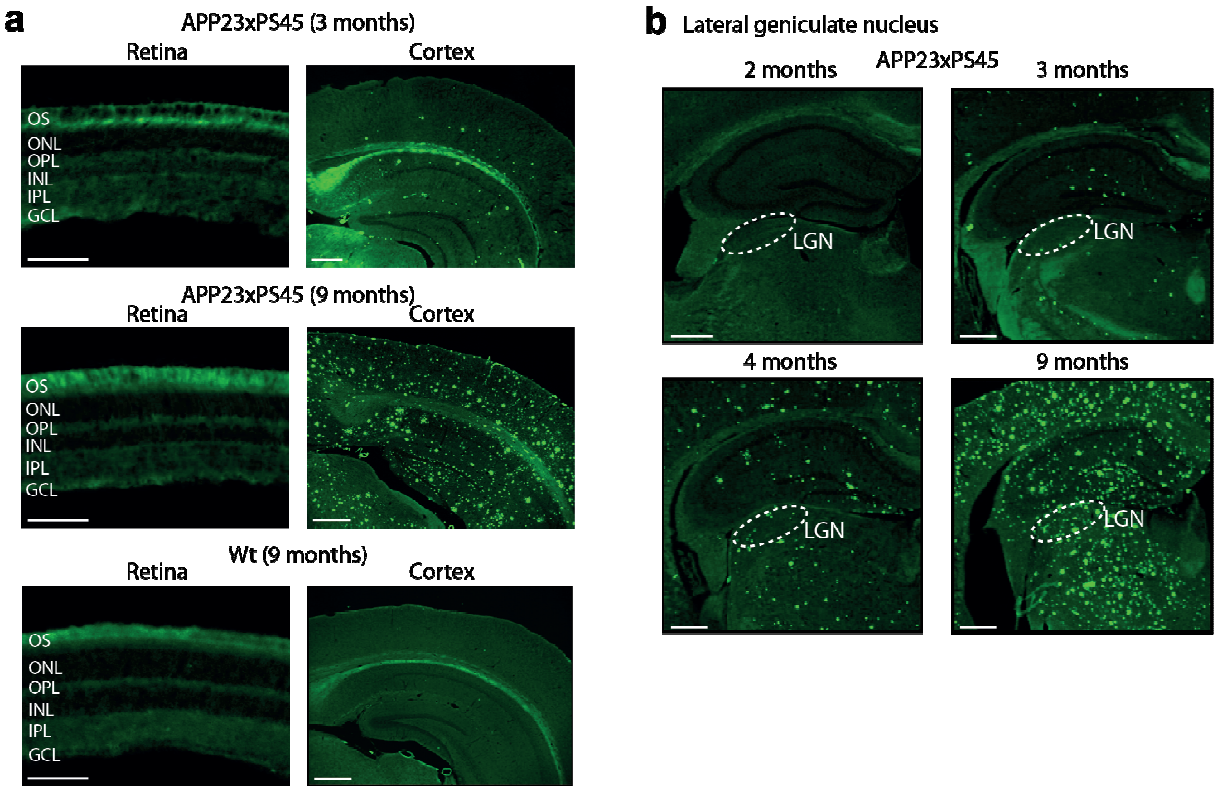

Supplementary Figure S1. Plaque density in the retina and the lateral geniculate nucleus. (**a**) Absence of amyloid-β plaques in the retina of 3 to 8-10-month-old APP23xPS45 mice. Micrographs of retinal (left panels) and visual cortex sections (right panels) stained with Thioflavin-S. The slices were obtained from a young APP23xPS45 mouse (3 months, upper panels), an aged APP23xPS45 mouse (9 months, middle panels) and an aged Wt mouse (9 months, lower panels), respectively. No plaques were found in the retina throughout all ages tested. The different retina layers are indicated. OS, outer segment of photoreceptors; ONL, outer nuclear layer; OPL, outer plexiform layer; INL, inner nuclear layer; IPL, inner plexiform layer; GCL, ganglion cell layer. (Scale bars, retina 100 µm, cortices 500 µm). (**b**) Development of amyloid-β plaques in the lateral geniculate nucleus (LGN) of APP23xPS45 mice. Micrographs of coronal slices of LGN stained with Thioflavin-S. The slices were obtained from APP23xPS45 mice of 2, 3, 4 and 9 months of age. The white dotted lines indicate the location of the LGN. Scalebars, 500 µm.

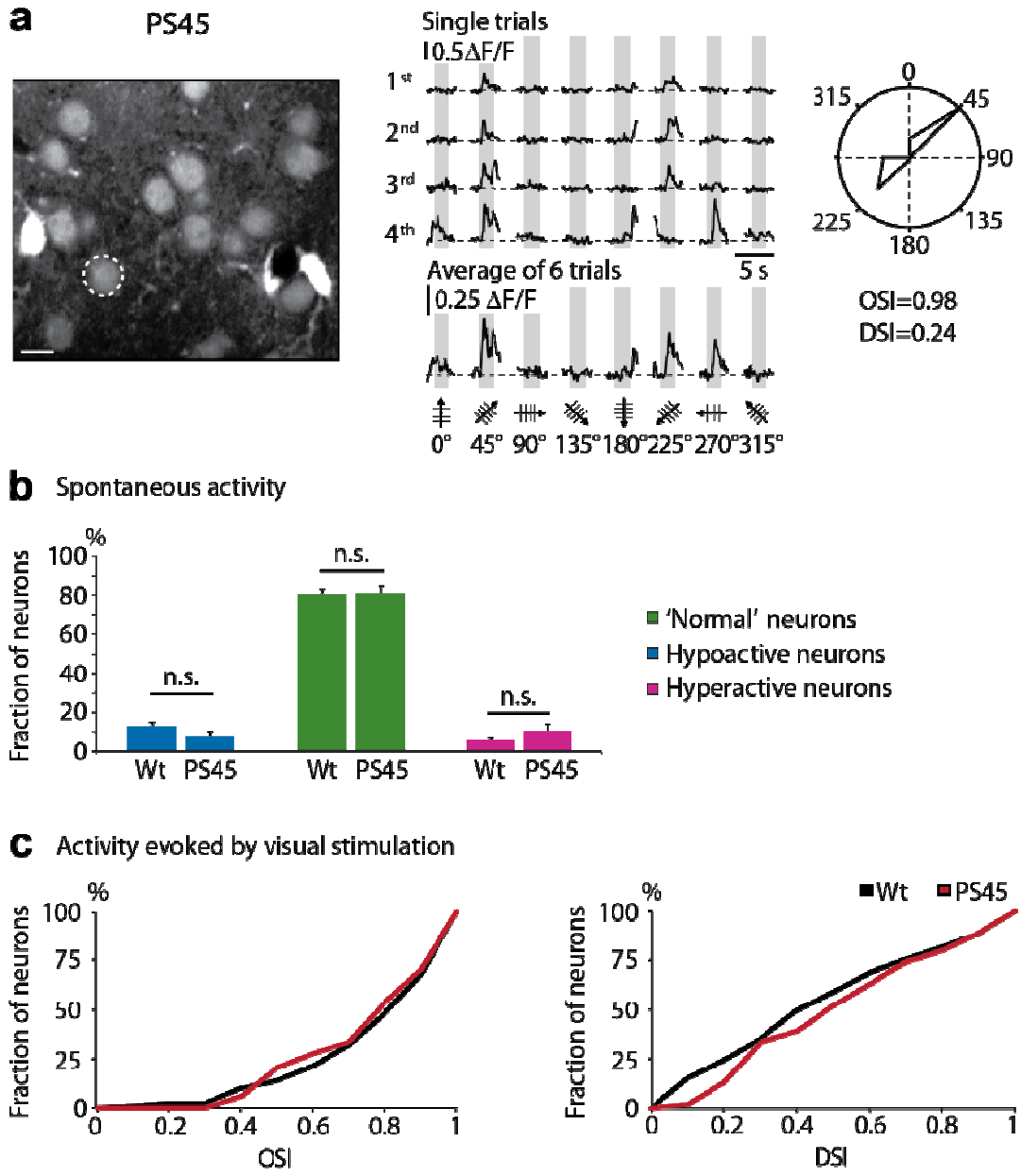

Supplementary Figure S2. Spontaneous activity, orientation and direction tuning of visual cortex neurons in the primary visual cortex of 8-10 month-old PS45 mice. (**a**) *Left panel*, in vivo two-photon image of layer 2/3 neurons in the visual cortex of a PS45 mouse (8 months). *Middle panel*, stimulus-evoked calcium transients recorded from the orientation selective neuron indicated in the left panel by a white dotted circle. Gray regions indicate periods of visual stimulation with drifting gratings schematized by oriented arrows on the bottom of each panel. Four single trials are represented on top and the average of 6 trials is shown below. Scale bar, 10 µm. *Right panel*, polar plot showing the neuron's response function to oriented drifting gratings.OSI, orientation selectivity index; DSI, direction selectivity index. (**b**) Bar graph showing the relative proportion of hypoactive, 'normal' and hyperactive neurons in 8-10-month-old Wt and PS45 mice (n=630 and 345 neurons in 15 and 5 mice, respectively). Error bars indicate SEM. (n.s., no significant difference, Mann-Whitney test; hypoactive, p=0.14; 'normal', p=0.93; hyperactive, p=0.27). (**c**) Cumulative distributions of the orientation (OSI) and direction (DSI) selectivity indices determined for all responsive neurons recorded in Wt (black; n=131 neurons in 13 mice) and PS45 (red; n=54 neurons in 4 mice) mice. No significant difference was found between Wt and PS45 mice (Mann-Whitney test; OSI, p=0.60; DSI, p=0.23).

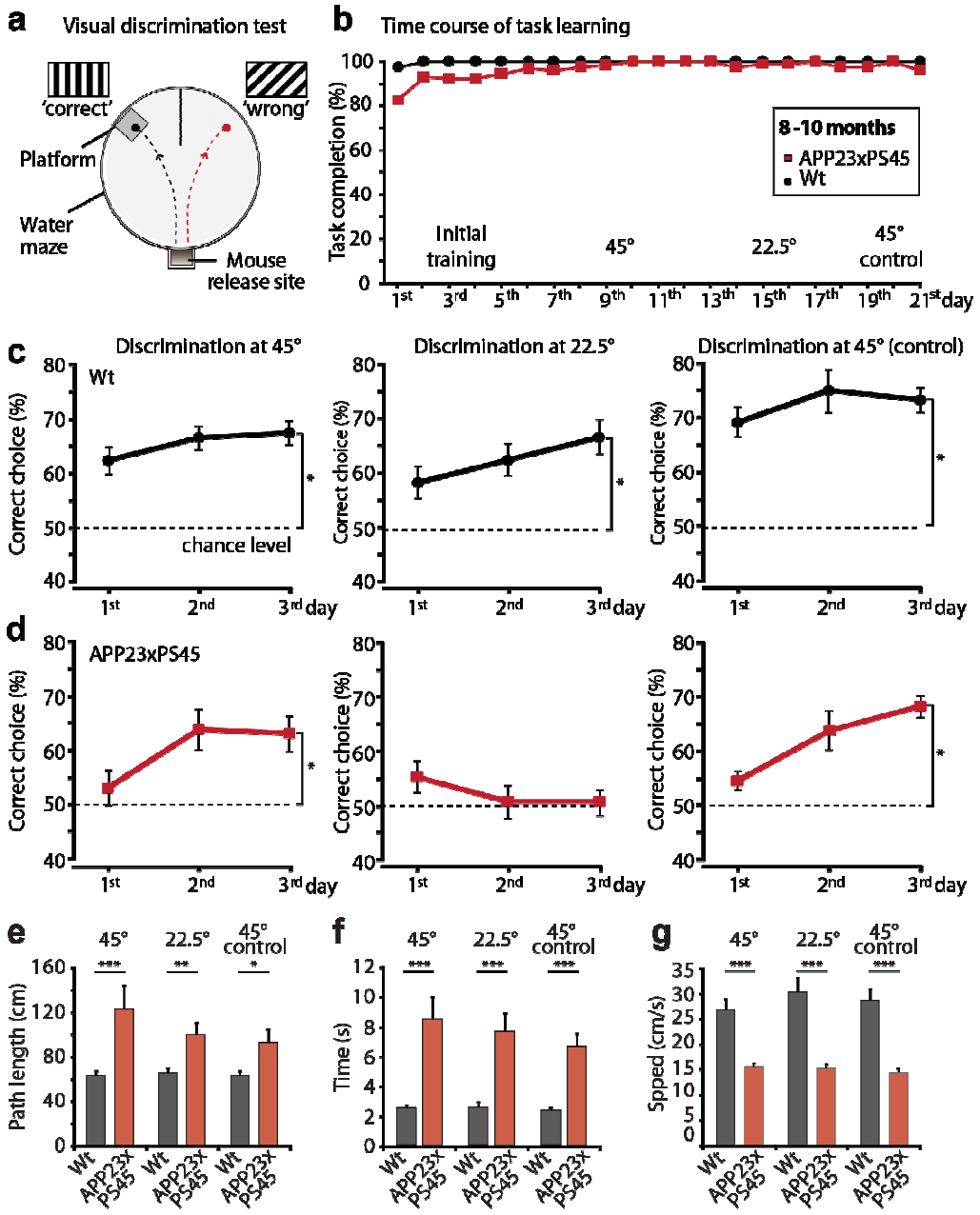

Supplementary Figure S3. Reduced visual discrimination in aged APP23xPS45 mice. (**a**) Schematic illustration of the visual pattern discrimination test. (**b**) Task learning development during the initial training and the testing phases. The task completion rate was estimated by the proportion of trials in which the mice reached either the platform located in front of the correct cue or the position of the platform in front of the wrong cue. (**c-d**) Mean percentages of the correct choices of Wt and APP23xPS45 mice during the visual discrimination test. *Left panels*, visual discrimination test illustrated in panel a (45° angle difference). The 50% chance level is indicated by a dotted line. Asterisks indicate a significant difference from the chance level: Chi-square test, Wt $p<0.001$ (n=12 mice), APP23xPS45 $p<0.005$ (n=13 mice). Error bars indicate SEM. *Middle panels*, the correct visual cue was still a vertically oriented drifting grating whereas the wrong choice was a clockwise 22.5° oriented one. The performance of the APP23xPS45 mice corresponded to the chance level (Chi-square, $p=0.861$), while Wt mice successfully learned the task (*$p<0.001$). *Right panels*, control visual discrimination test (45° angle difference) (Wt *$p<0.001$, APP23xPS45 *$p<0.001$). (**e-g**) Bar graphs showing the path length (e), the time spent to find the platform (f) as well as the swimming speed (g) of APP23xPS45 and Wt mice (8-10 months) during the 3 testing phases of the visual discrimination test. Note that all parameters were constant for both genotypes throughout the entire testing period (*$p<0.021$, **$p<0.005$, ***$p<0.001$).

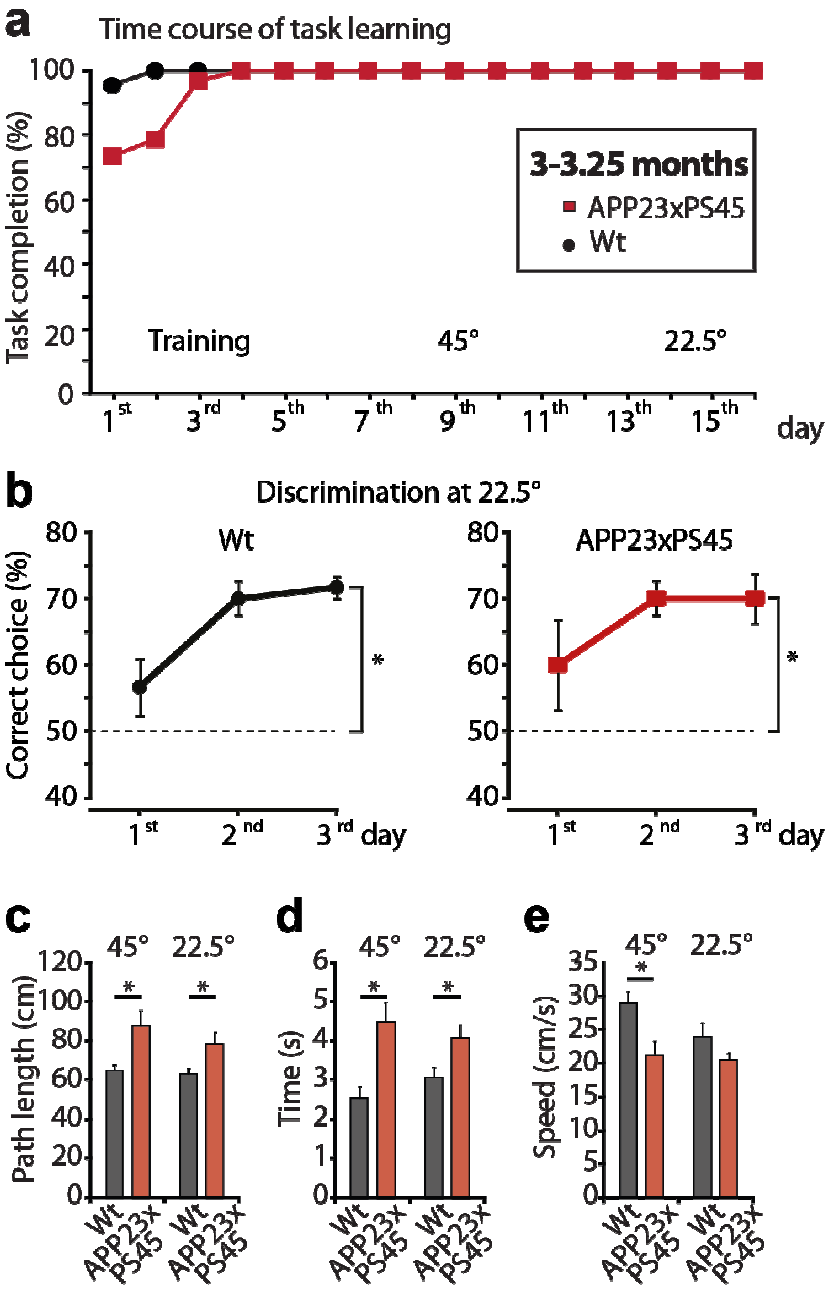

Supplementary Figure S4. Performance of young APP23xPS45 and Wt mice in the visual discrimination test. (**a**) Task learning development during the training and the testing phases. Same legend as Supplementary Figure S3a. (**b**) Mean percentages of the correct choices of Wt (left panel) and APP23xPS45 (right panel) mice determined for an angle difference of 22.5°. The 50% chance level is indicated by a dotted line. Asterisks indicate significant difference from chance level (Chi-square test; n=6 Wt, $p<0.005$; n=6 APP23xPS45, $p<0.005$). Error bars indicate SEM. (**c-e**) Bar graphs showing the path length (c), the time spent to find the platform (d) as well as the swimming speed (e) of young APP23xPS45 and Wt mice (3-3.25 months) during the two testing phases (orientation difference of 45°, 22.5°) of the visual discrimination test. Note that all parameters were constant for both genotypes throughout the entire visual tests. (Path length: 45° *$p<0.01$, 22.5° *$p<0.05$; Time: 45° *$p<0.001$, 22.5° *$p<0.05$; Swimming speed: 45° *$p<0.005$, 22.5° $p=0.35$).

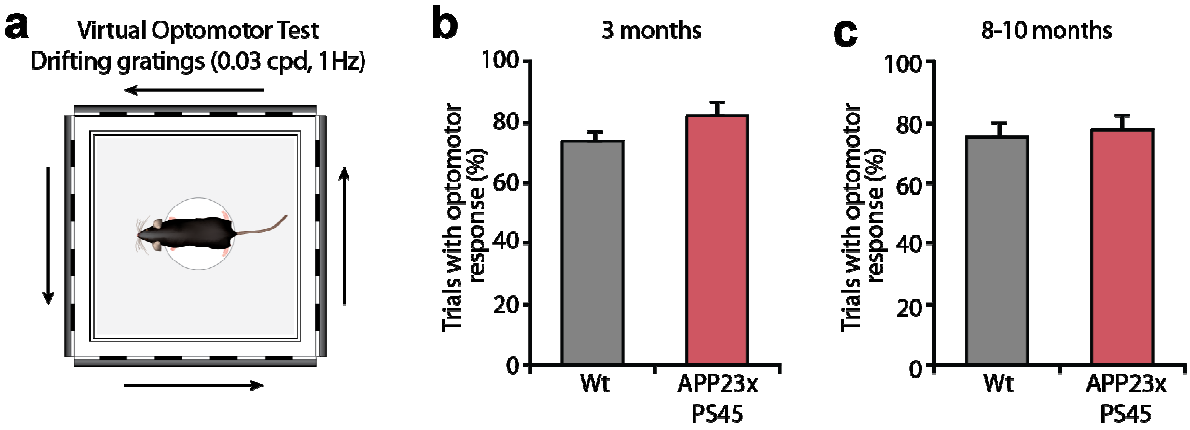

Supplementary Figure S5. Optomotor responses of APP23xPS45 and Wt mice. (**a**) Schematic illustration of the virtual optomotor system. The animal was placed on a platform, unrestrained, in the center of the arena. Rotating stimuli (square-wave vertical gratings, 1 Hz, contrast 80%, 0.03 cpd) were applied on the monitors, where they formed a virtual cylinder around the mouse. The direction of movements changed randomly. Mice responded to the stimuli by rotating their head following the direction of the moving gratings. (**b-c**) Bar graphs showing the percentage of trials with an optomotor response of young (3-3.25 months, panel c) and old (8-10 months, panel d) Wt (black; n=6 and 6 mice, respectively) and APP23xPS45 (red; n=6 and 6 mice, respectively) mice. No significant difference was observed between Wt and transgenic animals. Reliable optomotor responses have been shown to beassociated with normal retinal function[61]. These results indicate that both Wt and transgenic animals were able to see drifting gratings with the same spatial and temporal frequencies than that used for the visual discrimination test and the in vivo recordings.

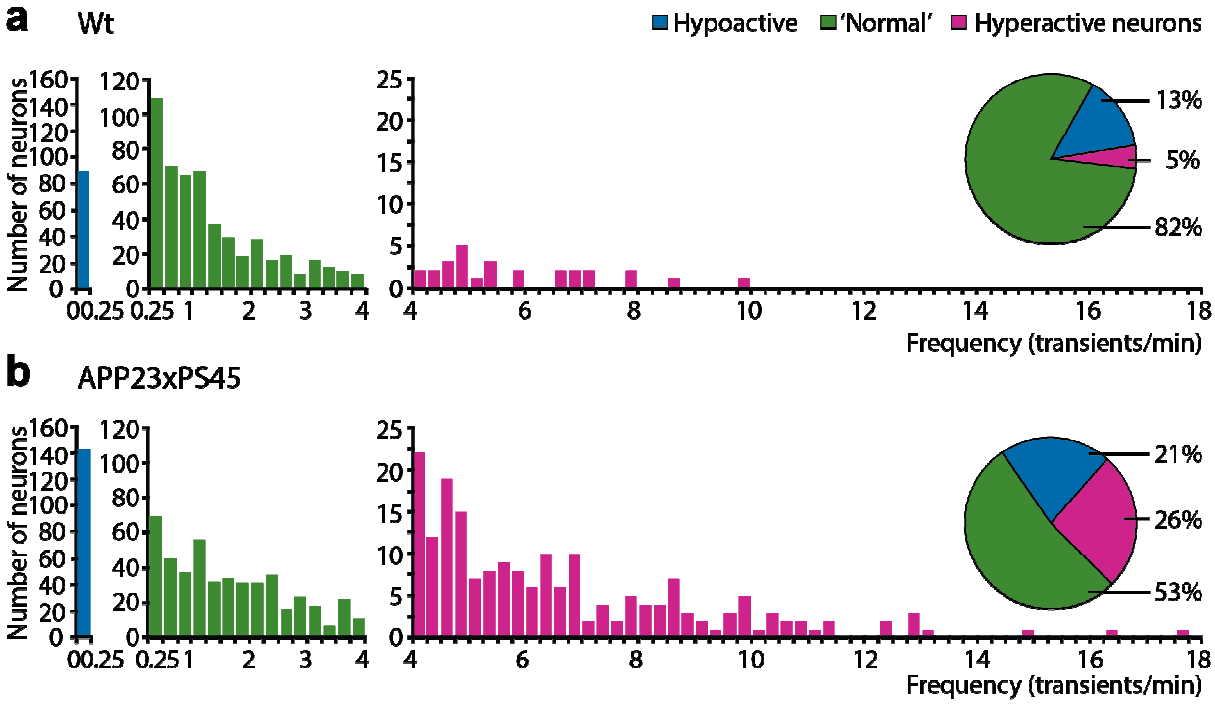

Supplementary Figure S6. Spontaneous activity in aged Wt and APP23xPS45 mice. (**a-b**) Frequency distribution of calcium transients during spontaneous activity of hypoactive (blue), 'normal' (green) and hyperactive (purple) neurons of APP23xPS45 and Wt mice (n=806 and 630 neurons in 19 and 15 mice, respectively). Spontaneous activity of each neuron was recorded during at least 4 min. Pie charts show fractions of hypoactive, normal and hyperactive neurons in Wt and APP23xPS45 mice.

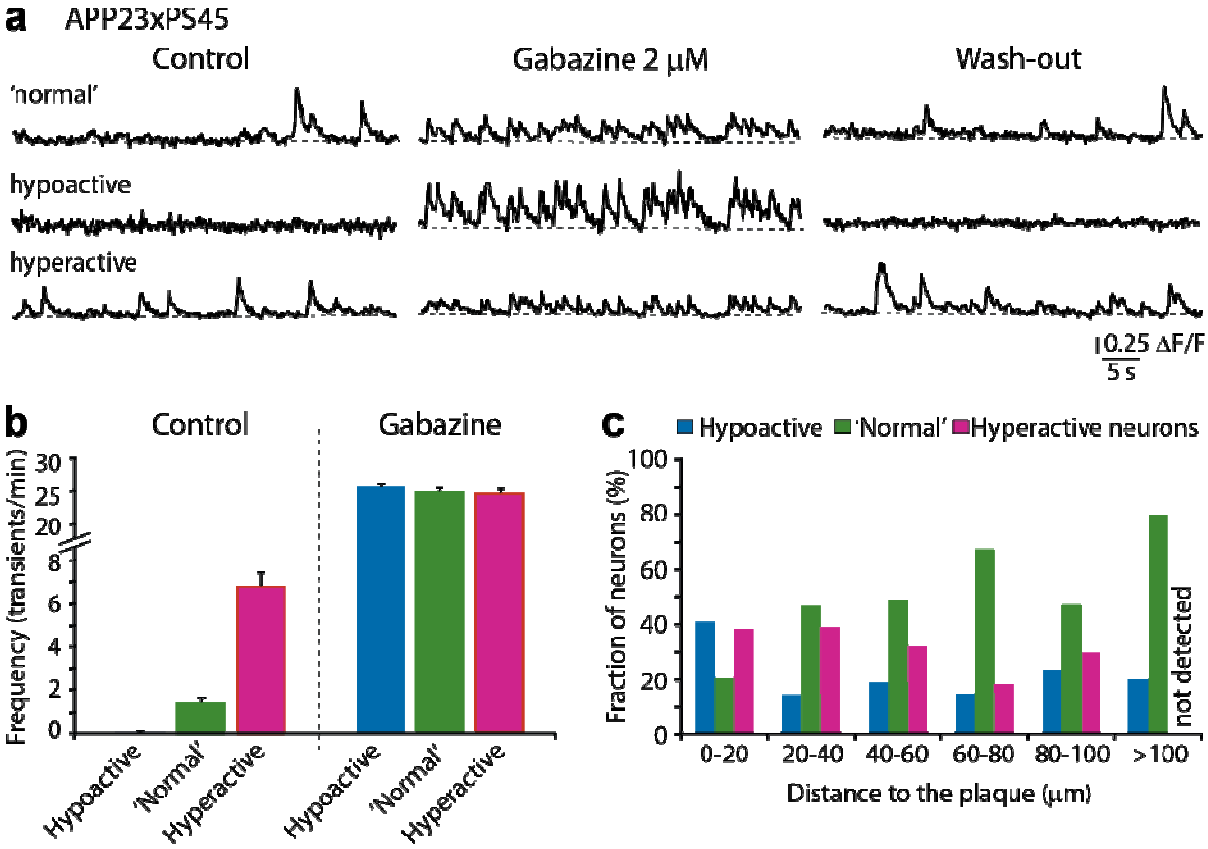

Supplementary Figure S7. Effect of $GABA_A$ receptor antagonist gabazine on spontaneous activity. (**a**) Spontaneous calcium transients before, during and after bath application of the $GABA_A$ receptor antagonist gabazine (2 µM) in layer 2/3 'normal', hypoactive and hyperactive neurons in the visual cortex of an APP23xPS45 mouse (8.5 months). (**b**) Summary graph illustrating the effect of gabazine on the frequency of calcium transients (n=6 hypoactive, 12 'normal', and 11 hyperactive neurons). Application of the $GABA_A$ receptor antagonist gabazine increased the frequency of calcium transients in all three types of neurons to the same level of 25 transients/min. However, the relative frequency increase in hyperactive neurons (2.8-fold) was distinctly smaller compared with the frequency increase in 'normal' neurons (17-fold). Error bars indicate SEM. (**c**) Bar graph showing the proportion of silent, normal, and hyperactive neurons at different distances from the border of the nearest plaque (n = 606 neurons in 17 APP23xPS45 mice, 8-10 months).

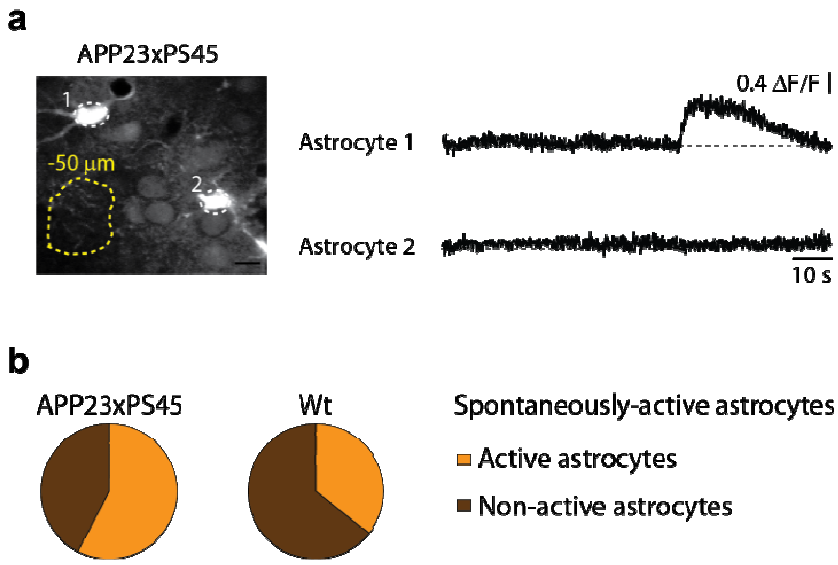

Supplementary Figure S8. Spontaneous activity of astrocytes in the primary visual cortex of aged Wt and APP23xPS45 mice. (**a**) Left panel, in vivo two-photon image of layer 2/3 neurons and astrocytes in the visual cortex of an APP23xPS45 mouse (8 months). The broken yellow line delineates a Thioflavin-S plaque observed 50 mm below the imaged focal plane. Right panel, spontaneous activity recorded from the astrocytes indicated in the left panel by a white dotted circle. Scale bar, 10 µm. (**b**) Pie charts representing the proportion of spontaneously active astrocytes in aged APP23xPS45 mice (57.5 %, n=66 astrocytes in 17 mice) and Wt mice (35 %, n=42 astrocytes in 14 mice). An astrocyte was considered active when at least one spontaneous calcium transient was recorded during the imaging period of spontaneous activity (at least 4 min).

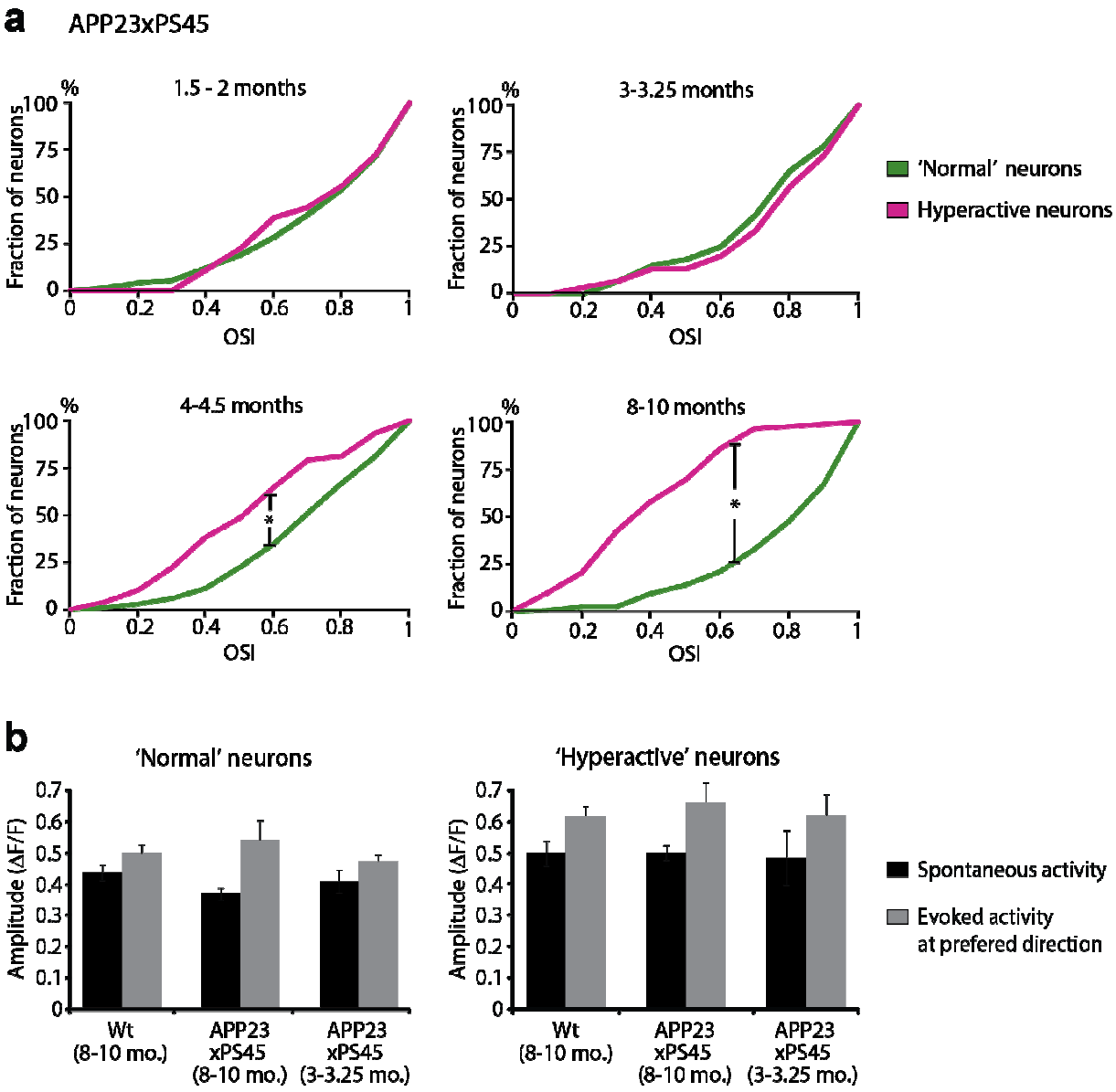

Supplementary Figure S9. Development of functional impairment of hyperactive neurons in the visual cortex of APP23xPS45 mice. (**a**) Cumulative distributions of orientation selectivity indices (OSI) determined for all responsive 'normal' (green) and hyperactive (purple) neurons recorded in APP23xPS45 mice at the four different ages (1.5-2, 3-3.25, 4-4.5, 8-10 months; n=74, 60, 97, 67 'normal' neurons and n=10, 30, 49, 78 hyperactive neurons in 7, 6, 8, 15 mice, respectively). Note that from the age of 4-4.5 months, hyperactive neurons have lower orientation selectivity compared to 'normal' neurons (Mann-Whitney test, 4-4.5 months *p<0.001; 8-10 months *p<0.001). (**b**) Peak amplitude of the spontaneous and evoked transients in Wt (8-10 months), APP23xPS45 (8-10 months) and young APP23xPS45 (3-3.25 months) mice. The peak amplitude of evoked activity was measured at the preferred direction. The response amplitude of normal and hyperactive neurons did not vary significantly between aged Wt and aged transgenic mice as well as between young (3 months) and aged (8-10 months) transgenic animals.

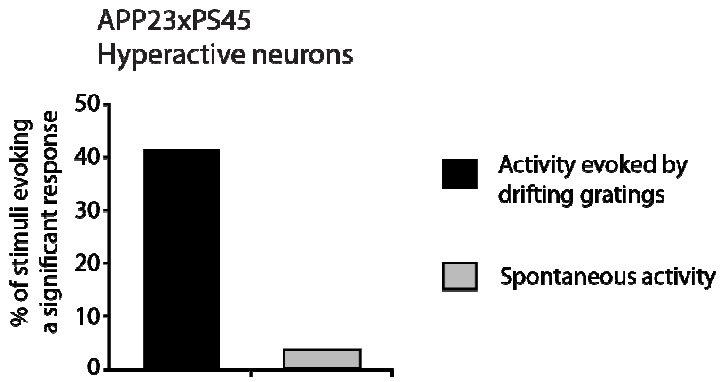

Supplementary Figure S10. Impact of high spontaneous activity on the detection of responses to drifting gratings in aged APP23xPS45 mice. ***Black bar***, percentage of significant responses to drifting gratings. Neuronal calcium responses evoked by drifting gratings were detected if their mean amplitude during the period of stimulation (2 s) was significantly above (t-test) the activity level during the preceding period (2 s). Using this analysis, hyperactive neurons in APP23xPS45 mice responded significantly to an average of 41.7 % of all drifting gratings. Thus, a hyperactive neuron was responding on average to 3.3 directions among the 8 directions of drifting gratings. ***Grey bar***, same analysis applied to recordings of spontaneous activity in the same neurons, after randomly assigning periods of nominal stimulation. A direction was randomly assigned to 8 epochs (2 seconds each) of the spontaneous activity trials. Then, an average of 6 trials was calculated. Finally, a t-test was performed between each of these epochs and the 2 seconds preceding them (equivalent to the standing grating periods in the evoked trials). Using this analysis, significant responses were detected in only 3.7 % of all stimuli epochs. Thus, for a given hyperactive neuron only a relatively minor fraction (< 9%) of false positive responses was detected in these conditions. The fact that hyperactive neurons in APP23xPS45 respond to many directions and have a low orientation tuning is thus not due to a simple increase in high spontaneous activity.

Supplementary Methods

Behavioral test, visual pattern discrimination task. The discrimination task was based on the same procedure described in a previous study[62,63]. In a circular water maze (diameter 80 cm, height 32 cm) filled with opaque water (23°C), animals had to locate a platform (10 x 10 cm) that was stable and kept invisible (about 5 mm submerged) in front of a specific visual cue (a grating with specific orientation) (see Supplementary Figure S3a). Visual stimuli were displayed on two identical computer monitors (1280 x 1024 pixels) that were placed along the maze on each side of a 25 cm long divider. Animals had to choose between two different visual cues. The platform was always placed below the correct visual cue computer screen (correct choice). Visual cues consisted of square-wave gratings (1 Hz, contrast 80%, 0.03 cpd as seen from the edge of the platform) and a mean luminance gray screen. Three groups of 8-month-old animals were tested independently (group 1: Wt n=6, APP23xPS45 n=5; group 2: Wt n=3, APP23xPS45 n=5; group 3: Wt n=3, APP23xPS45 n=3). In addition, one group of 3-month-old animals was tested (APP23xPS45 n=6, Wt n=6) with the same protocol.

The test consisted of four phases, the training phase and the three consecutive testing phases. For the first phase (training), the two visual cues were a gray screen (wrong stimulus) and a vertically oriented drifting grating (0°, correct stimulus). For the second phase, visual cues consisted of two drifting gratings of different orientations: a vertically oriented drifting grating (0°, correct stimulus) and a clockwise 45° oriented one (45°, wrong stimulus). For the third phase, the angle difference between both visual cues was reduced to 22.5° (0°, correct stimulus; 22.5°, wrong stimulus). Finally the fourth phase was identical to the second one (0°, wrong stimulus; 45°, correct stimulus). The understanding of the task was assessed during six initial training days (days 1-6). Then, phases 2 (6 days), 3 (6 days) and 4 (3 days) were added. Each day included 10 trials separated by 1-3 min inter-trial intervals. The position of the correct stimulus (left or right side of the divider) was changed pseudo-randomly. Mice were released into the maze from a box with a sliding door (see Supplementary Figure S3a). The percentage of correct choices was used to assess pattern discrimination performance. A correct choice was scored when the mouse touched the hidden platform. An incorrect choice was recorded when the mouse either reached the putative platform position on the wrong side (below the wrong stimulus) or failed to reach any platform position (correct or putative) within 30 s (error of omission). In case of an incorrect choice or an error of omission, animals were placed by the investigator onto the platform. All mice remained on this platform for about 5 s before being returned to their home cage. We verified that the mice were capable of completing the task by determining the proportion of trials in which the mice reached either the platform located in front of the correct cue (‘correct’ choice) or the position of the platform in front of the wrong cue (‘wrong choice’). At the end of the training phase, both Wt and APP23xPS45 mice reached a task completion rate higher than 96% and a level of correct choices significantly above the chance level (Chi-square test, Wt, $p<0.001$, APP23xPS45, $p<0.001$).

During the testing phases 2 and 3 the percentage of correct choices did not significantly change after the third day of testing, for both Wt and transgenic mice groups (Mann-Whitney test; 45° Wt p=0.132;APP23xPS45 p=0.866; 22.5° Wt p=0.254, APP23xPS45 p=0.675). Thus, we show in Supplementary Figure S3c-d, only the results of the first three days. All trials were video-taped with a digital camera (Sony, DCR-HC96E) mounted above the water maze for off-line analysis. Tracking of the swimming routes in the water

maze was performed with a custom-written software (LabView, National Instruments). We quantified the path length, the time spent to find the platform as well as the swimming speed. All these parameters were constant throughout the entire visual tests for both genotypes.

Measure of optomotor responses. The virtual optomotor system consisted of a square array of computer monitors placed at the four sides of a mirror with a side-length of 40 cm. The animal was placed on a platform, unrestrained, in the center of the arena. A camera (Sony, DCR-HC96E) was mounted above the animal in order to video-tape all trials. Rotating stimuli (square-wave vertical gratings, 1 Hz, contrast 80%, 0.03 cpd) were applied on the monitors, where they formed a virtual cylinder around the mouse[64]. Each session consisted of 20 trials, one trial lasting 15 sec. During the trials vertical drifting gratings were presented. The direction of movements changed randomly. The breaks between the trials also varied randomly between 8 and 30 sec. Mice responded to the stimuli by rotating their head following the direction of the moving gratings. Prior to testing the mice were adapted to the environment and arena by placing them on the platform for five minutes on three consecutive days. A session started by placing the animal on the platform while presenting resting gratings and left there for an adaptation period of five minutes. Only trials in which the mice showed no spontaneous movements were included in the evaluation. Sessions were repeated until at least 10 trials could be included into the evaluation. A positive trial was defined as a movement of the head into the same direction as the gratings. No head movements or head movements into the opposite direction were defined as negative trials. If, during the course of testing an animal slipped or jumped off the platform, it was simply returned to the platform and testing was resumed. Experimenters were blind to the genotype of the animals. The results are shown in Supplementary Figure S5. Both Wt and transgenic animals had reliable optomotor responses during the presentation of gratings with the same spatial and temporal frequencies than that used for the visual discrimination test and the *in vivo* recordings. These results indicate that both Wt and transgenic animals were able to see drifting gratings with such spatial and temporal frequencies.

Supplementary References

61. Thaung, C., Arnold, K., Jackson, I.J. & Coffey, P.J. Presence of visual head tracking differentiates normal sighted from retinal degenerate mice. *Neurosci Lett* **325**, 21-4 (2002).
62. Wong, A.A. & Brown, R.E. Age-related changes in visual acuity, learning and memory in C57BL/6J and DBA/2J mice. *Neurobiol Aging* **28**, 1577-93 (2007).
63. Prusky, G.T., West, P.W. & Douglas, R.M. Behavioral assessment of visual acuity in mice and rats. *Vision Res* **40**, 2201-9 (2000).
64. Prusky, G.T., Alam, N.M., Beekman, S. & Douglas, R.M. Rapid quantification of adult and developing mouse spatial vision using a virtual optomotor system. *Invest Ophthalmol Vis Sci* **45**, 4611-6 (2004).